

Deactivation of Nickel-Based Catalysts during CO Methanation and Disproportionation

C. MIRODATOS, H. PRALIAUD, AND M. PRIMET

Institut de Recherches sur la Catalyse, Laboratoire Propre du CNRS (conventionné à l'Université Claude Bernard, LYON I), 2 avenue Albert Einstein, 69626—Villeurbanne Cédex, France

Received December 11, 1985; revised March 27, 1987

The complex process of deactivation of Ni-based catalysts during CO methanation and disproportionation is studied by means of coupled kinetic and *in situ* physical methods (magnetism and infrared spectroscopy). Detailed analyses of the two main phenomena, namely metal sintering and carbon deposition, which contribute simultaneously to the overall deactivation are provided. The initial dispersion, the composition and pressure of the methanation feed, and the ability of the support to favor the water gas shift reaction are shown to play major roles in both the sintering mechanism and the surface poisoning by carbon. © 1987 Academic Press, Inc.

INTRODUCTION

Loss of metal surface area by poisoning, coking, or sintering is a serious problem in a number of processes involving Ni catalysts. High temperature processes on Ni metal catalysts are particularly affected by sintering of the particles. However, other parameters such as the surrounding gases may also affect the catalyst sintering; for instance, metal carbonyl formation (1, 2) and low temperature methanation can also result in growth of Ni particles. The extensive published data dealing with carbon deposition have been reviewed by Mills and Steffgen (3), Rostrup-Nielsen (4), Trimm (5), and more recently by Bartholomew (6) and by Wolf and Alfani (7). In spite of the absence of massive C deposition on Ni catalysts (3, 8), blocking of active sites may occur under methanation conditions.

The deactivation of Ni-based catalysts for low temperature methanation has often been studied with particular focus on one of the deactivation processes, carbon deposition, metal sintering, or sulfur poisoning. In this work, as a first stage, we report a study of the two first-mentioned aging phenomena, namely metal sintering and carbon deposition, under the usual condi-

tions of low temperature methanation on a series of nickel catalysts. The two phenomena occur simultaneously.

Both catalytic reaction and physical characterization of the catalysts were carried out in order to determine the actual changes in the nickel state and the adsorbed species which may cause the deactivation. As it is known that the properties of nickel catalysts are influenced by the support or by the presence of additives, several supports have been considered: SiO₂, MgO, Al₂O₃, Cr₂O₃, MgSiO₃, and MgAl₂O₄. Additives (chromium, molybdenum, potassium) have also been added to a silica-supported Ni solid. In the present paper three supports SiO₂, Al₂O₃, MgO and one additive (potassium) have been selected, each of them illustrating well the different types of deactivation which were observed with the whole series of catalysts.

EXPERIMENTAL

Materials

The precursors were obtained by contacting the supports (SiO₂, MgO, Al₂O₃) with a nickel nitrate hexammine solution. After decomposition of the complex, supported Ni(OH)₂ was formed (9). In order to

obtain the doped solids the precursor $\text{Ni}(\text{OH})_2/\text{SiO}_2$ was added to a solution of KNO_3 and stirred (10). The water was evacuated to dryness under reduced pressure at 353 K in a rotary evaporator. All the precursors were dried at 393 K for 15 h.

Reductions were carried out overnight in flowing hydrogen (4 liters h^{-1}) with a linear increase in the temperature up to the required value at the heating rate of 2 K min^{-1} . As the reducibility depends on the nature of the support, the final reduction temperature was low enough to avoid strong metal support interaction (SMSI) and high enough to obtain a reduction as complete as possible and to minimize any interaction between the metallic phase and the unreduced one (11). Table 1 lists some characteristics of the selected solids.

Magnetism

Degrees of Ni reduction were deduced from saturation magnetization measurements of the outgassed samples (1.3×10^{-4} Pa, 700 K for 2 h) using the Weiss extraction method (12). Average Ni particle diameters (Table 1) were calculated from the Langevin low and high field methods for superparamagnetic samples (12). During adsorption or reaction, the Ni atoms involved in chemical bonding cease to partici-

pate in the collective ferromagnetism (12). The changes in saturation magnetization then led to the magnetic "bond number" n .

It was possible to perform magnetic measurements after the methanation reaction without exposure to air and at various pressures (0.1 to 2 MPa) with a high pressure stainless-steel cell.

Surface average diameters of Ni particles were also obtained from hydrogen chemisorption measurements using a classical volumetric apparatus equipped with a pressure gauge. Some samples, especially the nonsuperparamagnetic ones, were also examined in a transmission electron microscope. For fully superparamagnetic solids (Table 1) a good agreement between diameters deduced from the various methods was achieved. For partially superparamagnetic samples, e.g., sintered catalysts, the most reliable data were obtained from TEM.

Infrared Spectroscopy

For infrared experiments, the precursors were compressed under 4 tons cm^{-2} pressure in order to obtain disks (1.8 cm in diameter, weight comprised between 30 and 50 mg). The infrared spectra of CO adsorbed on *in situ* reduced and outgassed samples were run on a Fourier transform spectrometer (Bruker IFS 110). The spectra

TABLE I
Morphological Characteristics of the Catalysts after Reduction

Solids	Ni (wt%)	Potassium additive (wt%)	Reduction temperature (K)	Reduction level (%)	Average ^a diameter (nm)
Ni/SiO ₂	20.1	0	923	100	4.2
Ni/MgO	17.4	0	973 ^b	80	7.8
Ni/Al ₂ O ₃	21.1	0	923	100	7.0
Ni-K/SiO ₂ ^c	23.2	2.5	923	100	6.0

Note. Supports: SiO₂ (Degussa) 200 m²/g; Al₂O₃ (Degussa) flame method, 100 m²/g; Mg(OH)₂ from MgCl₂ + KOH, 117 m²/g.

^a Average diameters deduced from magnetic measurements.

^b As the reduction of catalysts containing magnesia presents some problems we have verified that the reduction level of the magnesia-supported Ni solids does not alter the properties here reported.

^c The chemical state of the potassium additive is discussed in Refs. (10, 16).

were computed from accumulated spectra recorded before and after adsorption (4 cm^{-1} resolution, 200 scans) and ratioing both spectra. Changes in the surface-adsorbed species following adsorptions or methanation were also followed in a heatable cell (14).

Catalytic Activities

After *in situ* reduction of the catalysts, the carbon monoxide hydrogenation (flowing $3\text{H}_2 + \text{CO}$ mixture, 1.5 liters h^{-1}) was performed at atmospheric pressure using a fixed bed differential dynamic reactor. The effluents were analyzed in a gas chromatograph equipped with catharometric detection. In typical experiments the solids were compared for the same reaction temperature (507 K) and for similar initial conversions (between 3 and 8% of CO converted). The space velocities ranged from 30 to 40 liters $\text{g}^{-1} \text{h}^{-1}$. The deactivation runs were stopped after various times on stream in order to determine the changes in particle size and the amounts of carbon deposited on the solids. It was also possible to perform the reaction at various temperatures between 473 and 600 K and at pressures up to 2 MPa. For this latter case a high pressure stainless-steel cell allowing both a kinetic study in flowing conditions and *in situ* magnetic measurements was used. The reaction of CO disproportionation was also performed in order to discard the possible effects of H_2 in deactivation processes. In this case the catalytic activity was evaluated from the conversion of CO into CO_2 according to the reaction



Temperature-Programmed Reactions

Temperature-programmed hydrogenations of carbon deposits (TPH) were performed, methane being the main gaseous product. After standard deactivation experiments, the catalysts were cooled to room temperature in flowing helium and then heated at a programmed rate (8 K min^{-1}) up

to 923 K in flowing hydrogen (3.6 liters h^{-1}). The methane concentration was plotted against the programmed temperature.

The carbon deposits were also reacted with carbon dioxide as follows. After methanation, hydrogen was admitted at the reaction temperature in order to remove the "active" carbon deposits (see further below). After purging with helium the catalysts were contacted with flowing CO_2 (1.1 liters h^{-1}) at the reaction temperature. Carbon monoxide evolution was measured. Chemical analyses of the carbon deposits after reaction were also performed after treatment with flowing hydrogen at 507 K.

RESULTS AND DISCUSSION

CATALYTIC ACTIVITIES

The overall deactivation which occurs during the methanation reaction at atmospheric pressure with the selected solids is presented in Fig. 1. The curves report the normalized activities versus time on stream. Normalized activity is defined as the ratio of the instantaneous activity A_t to the initial one A_0 , A_t and A_0 being expressed by the number of CO molecules converted into hydrocarbons (and CO_2) per second and per square centimeter of active surface.

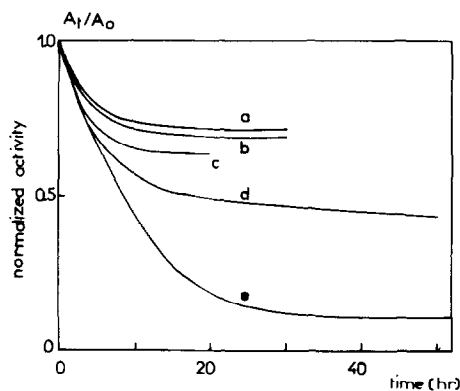


FIG. 1. Normalized activity A_t/A_0 vs time on stream. Curve a, Ni/ Al_2O_3 ; curve b, Ni/ MgO ; curve c, Ni-K/ SiO_2 , conversion, 8%, selectivity toward CO_2 , 32%; curve d, Ni-K/ SiO_2 , conversion, 3%, selectivity toward CO_2 , 18%; curve e, Ni/ SiO_2 . Curves a, b, e, reaction temperature, 507 K. Curves c, d, reaction temperature, 573 K.

Let us first concentrate on the three solids Ni/SiO₂, Ni/MgO, Ni/Al₂O₃ for which the deactivation has been studied under the same reaction conditions. The initial activities at 507 K are respectively 1.2×10^{13} , 2.3×10^{13} , 4.1×10^{13} molecules s⁻¹ (cm² Ni)⁻¹. No changes in the rate of deactivation are observed as a function of the initial degree of conversion (which is monitored by the weight of catalyst and the overall flow rate for given *T*, *P* conditions). As already shown and discussed in Ref. (11), the selectivities toward methane and higher hydrocarbons vary with the support (96% of the CO converted is CH₄ for Ni/SiO₂, 81% for Ni/MgO, and 60% for Ni/Al₂O₃). Furthermore, the selectivity toward CO₂ increases with the support basicity and with the reaction temperature. For instance, for Ni/MgO, 2 to 4% of the CO converted is CO₂ at 507 K and 8% at 543 K. We will only emphasize that in no case do the selectivities vary upon deactivation. The curves of Fig. 1 and the values at *t*_{0.5} or *t*_{0.2} (times for which the activity equals 50 or 20% of the initial activity) show that the overall deactivation is very important for Ni/SiO₂. By contrast the Ni/MgO and Ni/Al₂O₃ solids display a much more stable activity.

Concerning the Ni-K/SiO₂ solid, the addition of potassium to Ni/SiO₂ is already known to decrease the methanation rate strongly (15, 16). Hence to reach similar conversions the reaction has been performed at higher temperatures (Fig. 1), the initial activity thus being equal to 2.8×10^{12} molecules s⁻¹ (cm² Ni)⁻¹ at 573 K. In this particular case, even in the range of conversions studied (3–8%) greater quantities of CO₂ are observed at higher CO conversions, as already noticed by Moeller and Bartholomew for Ni-Mo solids (17). This is assigned to the water gas shift reaction (WGS)



since the WGS reaction rate is a positive function of the partial pressure of water and since the concentration of water produced

by the methanation increases with the conversion. At the same time the rate of deactivation decreases as the initial conversion (and the selectivity toward CO₂) increases (Fig. 1). We will return later to this particular point by studying the influence of CO₂ partial pressure in the reactant mixture.

The effect of pressure on the deactivation both in the methanation and in the disproportionation reactions has been studied on the Ni/SiO₂ solid (Fig. 2). When increasing the total pressure up to 1 MPa the decay of the methanation rate is faster for around the first 10 h (*A*_{10h}/*A*₀ = 0.45 for 0.1 MPa and 0.20 for 1 MPa) but tends to be pressure independent after 20 h on stream. Concerning the reaction [1], 2CO → C + CO₂, in the absence of hydrogen, the overall deactivation is faster and larger than that for methanation and increases with the CO pressure (0.1 MPa, *A*_{10h}/*A*₀ = 0.1; 0.5 MPa, *A*_{6h}/*A*₀ = 0).

Since no sulfur compound is present in the feed, the decreases in activity observed in this study are assigned to carbonaceous deposits and/or to metal sintering. Both processes of deactivation are successively analyzed.

NICKEL SINTERING

The occurrence of metal sintering during the reaction of methanation is clearly dem-

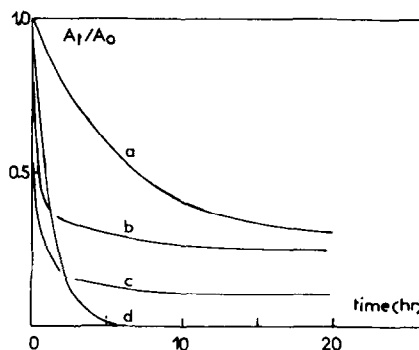


FIG. 2. Normalized activity *A*_{*t*}/*A*₀ vs time on stream for the Ni/SiO₂ solid. Curve a, methanation at 0.1 MPa; curve b, methanation at 1.0 MPa; curve c, disproportionation at 0.1 MPa; curve d, disproportionation at 0.5 MPa.

onstrated in Figs. 3 and 4 which report the changes in particle diameters as a function of time on stream, for various catalysts, feed composition, and pressure.

As shown in Fig. 3, the Ni/SiO₂ sample displays the largest trend to sinter, inasmuch the initial particle size is small. This is the case for the sample reduced at mild temperature (curve a) which initially shows a high metal dispersion and a narrow distribution of particle sizes centered around 4 nm. After 20 h on methanation stream this sample is heterodispersed because it displays not only spherical superparamagnetic particles of average size 8 nm but also some kinds of rafts of ca. 10 nm (thickness) × 25 nm (width) × 60 nm (length) detected by electron microscopy. By contrast, starting from samples poorly dispersed but nevertheless presenting a narrow distribution of particle sizes (Ni/Al₂O₃, Ni/MgO, Ni-K/SiO₂, or high temperature reduced Ni/SiO₂) the sintering phenomenon is much more limited (Fig. 3) and the final size distribution remains narrow (average size, 8 nm).

Considering now the effect of feed composition and pressure (Fig. 4), it looks obvious that there is a straightforward rela-

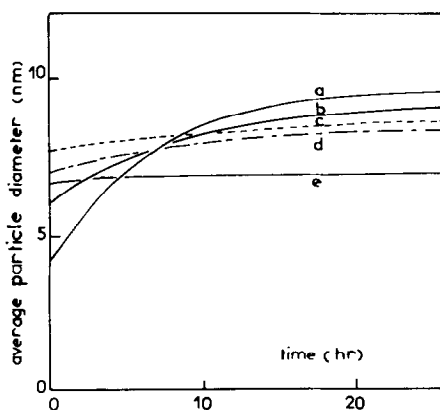


FIG. 3. Changes in average particle diameter vs time on stream in methanation at 498 K with Ni/SiO₂ reduced at 923 K (a); Ni/SiO₂ reduced at 1103 K (b); Ni/MgO reduced at 973 K (c); and Ni/Al₂O₃ reduced at 923 K (d) and in methanation at 559 K with Ni-K/SiO₂ reduced at 885 K (e). The average particle diameters reported here correspond to the superparamagnetic particles (magnetic measurements).

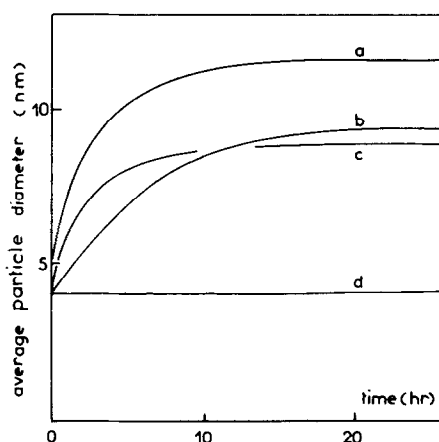


FIG. 4. Changes in average particle diameter vs time on stream for Ni/SiO₂ catalysts as a function of the feed composition and pressure. (a) 3H₂ + CO, 2.1 MPa; (b) 3H₂ + CO, 0.1 MPa; (c) CO, 0.1 MPa; (d) H₂ + H₂O, 0.1 MPa.

tion between the CO pressure and the rate and extent of sintering, whereas hydrogen and water partial pressures do not induce any sintering process at the methanation temperature.

From these observations one can easily conclude that the sintering of nickel which is observed in the presence of CO proceeds via the formation of nickel carbonyl species in agreement with the work of Shen *et al.* (2). As (i) no loss of material is observed even after severe sintering, (ii) the nickel transport occurs at temperatures far below the temperature of spontaneous migration of metal particles (the Tamman temperature is 946 K for Ni), and (iii) this process is favored by a high nickel dispersion and a low temperature of reaction, a plausible mechanism of nickel sintering is the migration of molecular nickel carbonyl, probably along the surface. This is consistent with the observations of van Meerten *et al.* (1) and could be related to the general model of interparticle transport proposed by Wanke and Flynn (18). More quantitatively, the changes in nickel dispersion, D (a reverse function of particle diameter), versus time on stream can be satisfactorily described by the power law rate equation,

$-dD/dt = k_D P_{CO} D^3$, following the Levenspiel concept of parallel deactivation.

This loss of active surface with time on stream accounts for most of the overall deactivation which is observed on the various catalysts during the first 15 h on stream. Particularly, it explains well the fast decay of activity observed with the well-dispersed Ni/SiO₂ solid during the first period of reaction (Fig. 1), this being still more pronounced when the CO partial pressure is increased 20-fold. Later on, the phenomenon of nickel sintering stabilizes. This corresponds probably to an equilibrium of formation/migration/decomposition of the carbonyl species between the nickel particles. Nevertheless, the deactivation still proceeds, although at a lower rate: another process must be invoked to account for the overall deactivation. This statement that the nickel sintering occurs mainly in the first period of reaction with a fresh and well-dispersed catalyst will lead us to study the carbon deposit phenomena on "used catalysts" (after ca. 15 h on stream).

CARBON DEPOSITS

The amounts of carbon which are formed on the solids during the reaction vary largely with the time on stream and the type of catalyst. Table 2 shows the amount of C (determined by chemical analysis) deposited on the selected catalysts at different stages of reaction. This amount is quite high in the case of Ni/Al₂O₃, Ni/MgO, Ni-K/SiO₂ and it increases with time.

By means of temperature-programmed hydrogenation, at least three types of carbon deposit formed during the methanation are detected (Fig. 5). They are referred to as low, intermediate, and high temperature species, respectively. The effects of support, reaction time, and pressure on the formation of these carbon species and the related changes in the magnetic properties of nickel have been studied. The deposited amounts are evaluated for each type of carbon and reported in Table 2.

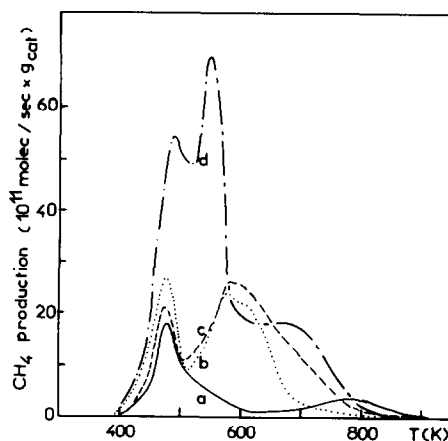


FIG. 5. Temperature-programmed hydrogenation (8 K min⁻¹) of carbon deposits after methanation during 15 h at 507 K on Ni/SiO₂ (a), Ni/Al₂O₃ (b), and Ni/MgO (c), and at 559 K on Ni-K/SiO₂ (d). Changes in methane concentration with temperature.

(i) Low Temperature Species

For nickel supported on various supports, without additive, a first peak of methane is observed at temperatures below 523 K which corresponds, therefore, to the most reactive species. As a matter of fact this carbon species is eliminated by a treatment in flowing hydrogen at the reaction temperature (507 K). The amount of this species is little affected by the reaction time, is nearly pressure independent, and does not vary significantly with the support (Table 2, species I). This species increases when the temperature is decreased during the methanation reaction. Magnetic measurements performed *in situ* during methanation show a decrease in the saturation magnetization of around 8–10% after 2 h. Afterward no change in saturation magnetization is observed. The initial value is restored by a hydrogen treatment at 573 K. Determination of the bond number ($n_c = 3$) shows that three Ni surface atoms cease to participate in the collective ferromagnetism per atom of C added. This is consistent with the Ni₃C surface carbide species postulated as the active intermediate in methanation (19, 20). We call this first type of carbon "reactive carbon." It may be related to the

TABLE 2
Amounts of Carbon (Percentage of Sample Weight) Formed during
the Methanation Reaction

Samples	CO ₂ pressure in the feed (kPa)	Time on stream (h)	Chemical analysis ^a	TPH		
				I	II	III
Ni/SiO ₂	0	2	0.008	0.085	—	0.009
		15	0.05	0.099	—	0.044
		49	0.19			
		66	0.25			
	3.1	15		0.1	—	0.009
		49	0.11			
Ni/Al ₂ O ₃	0	15	0.50	0.090	0.469	—
Ni/MgO	0	15	1.7	0.067	0.620	—
Ni-K/SiO ₂ ^b	0	15	0.75	0.87 ^c	0.44	—

Note. Reaction temperature: 507 K for Ni/SiO₂, Ni/Al₂O₃, Ni/MgO; 573 K for Ni-K/SiO₂.

^a Carried out after treatment under a hydrogen flow at the reaction temperature for 1 h after elimination of the active carbon (peak I).

^b Conversion 8%; selectivity toward CO₂, 32%.

^c Surface + bulk carbide as discussed in the text.

C_α species described by McCarty and Wise (21) and discussed by Bartholomew (6). Let us recall that if during methanation the formation of Ni carbide is restricted to the surface of the Ni particle, interstitially dissolved carbon rapidly transformed into bulk carbide is observed during disproportionation (22). Geus and co-workers have also found that Ni₃C strongly changes the magnetic properties of nickel (23).

For the potassium-containing solid (Fig. 5, curve d), two peaks instead of one are observed at low temperature. The first one at 500 K corresponds to the surface Ni₃C as for the other catalysts. The second one, very large, at 550 K is assigned to bulk nickel carbide since the related amount of carbon, evolving as methane, implies a carbidization of ca. 70% of the nickel loading, which agrees very well with the 66% decrease in the sample magnetization noted after the CO/H₂ reaction. It has been stated that the surface carbide formed from the CO dissociation can either react into methane or dissolve interstitially into bulk carbide, i.e., can undergo two competing reactions (22). The tendency for Ni-K/SiO₂ samples to form bulk carbide can therefore

be simply explained by the low methanation activity which favors the carbidization.

(ii) Intermediate Temperature Species

The adsorption of CO has been followed at room temperature by infrared spectroscopy on the selected samples. The hydrogenation of adsorbed carbon monoxide was studied as a function of the temperature.

Ni/SiO₂ catalyst. Adsorption of CO at 300 K leads to the appearance of ν CO bands at 2060–2030, 1930, and 1850 cm⁻¹, respectively attributed to CO bonded to one, two, and four nickel surface atoms (24, 25) (Fig. 6). By contacting the previous sample with hydrogen under a 33.3 kPa pressure at 300 K, the ν CO bands due to the linear form become sharper and are shifted toward higher wavenumbers (2075 cm⁻¹); the distribution of the CO molecules multi-bonded to nickel is also modified; i.e., the bands due to the bridged species almost completely disappear whereas the Ni₄CO species grow. By heating under hydrogen at 423 K, the linear forms remain unaffected. On the contrary, the most reactive multi-bonded CO species progressively disappear and their ν CO frequencies are continuously

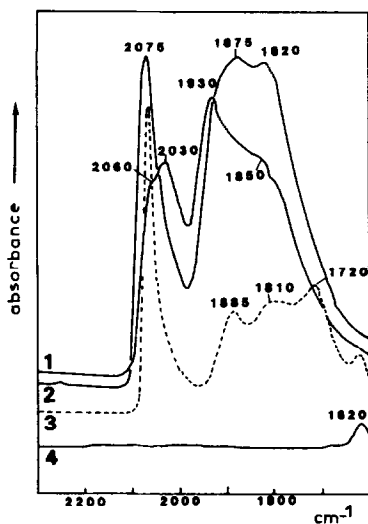


FIG. 6. Ni/SiO₂. Infrared spectroscopy. Range 1600–2300 cm⁻¹. (1) Irreversible chemisorption of CO at room temperature. (2) After CO chemisorption, hydrogen treatment (33.3 kPa) during 17 h at room temperature. (3) Hydrogen treatment (33.3 kPa) 1 h at 423 K. (4) Hydrogen treatment 1 h at 473 K.

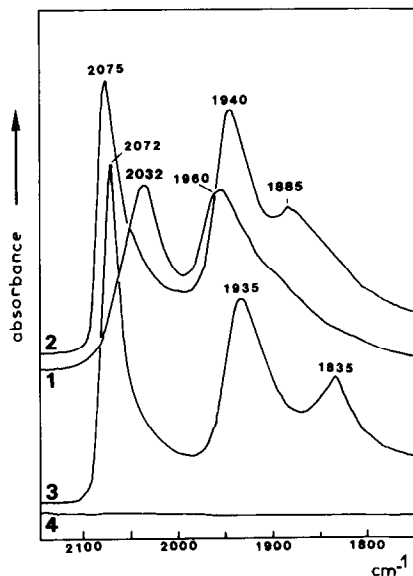


FIG. 7. Ni/Al₂O₃. Infrared spectroscopy. Range 1800–2100 cm⁻¹. (1) Irreversible chemisorption of CO at room temperature. (2) Hydrogen treatment (13.3 kPa) during 16 h at room temperature. (3) H₂ (13.3 kPa) 1 h at 373 K. (4) H₂ (13.3 kPa) 1 h at 473 K.

shifted toward lower wavenumbers in accordance with a stronger interaction of the remaining CO molecules with the surface nickel atoms. After heating at 473 K under hydrogen, adsorbed carbon monoxide is fully converted into methane, no intermediate species linked or not to the support being observed.

Ni/Al₂O₃ catalyst. As for the Ni/SiO₂ sample, irreversible adsorption of CO at 300 K leads to the formation of linear ($\nu\text{CO} = 2032 \text{ cm}^{-1}$), bridged ($\nu\text{CO} = 1960 \text{ cm}^{-1}$), and multicentered species ($\nu\text{CO} = 1885 \text{ cm}^{-1}$). The intensity of the latter band is very weak (Fig. 7). In addition, bands due to hydrogen-carbonate species (1650, 1460, 1230 cm⁻¹) (26) linked to the support are observed (Fig. 8). The addition of hydrogen (pressure = 13.3 kPa) at 300 K on the CO-covered sample leads to the following changes:

- sharpening and shift of the 2032-cm⁻¹ band to 2075 cm⁻¹,
- increase in the intensity of the band due to Ni₄CO groups,

—increase in the intensity of the bands due to hydrogen-carbonate species.

Heating at 373 K under hydrogen does

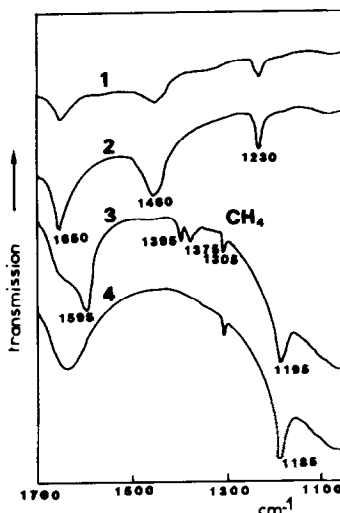


FIG. 8. Ni/Al₂O₃. Infrared spectroscopy. Range 1100–1700 cm⁻¹. (1) Irreversible chemisorption of CO at room temperature. (2) Hydrogen treatment (13.3 kPa) during 16 h at room temperature. (3) H₂ (13.3 kPa) 1 h at 373 K. (4) H₂ (13.3 kPa) 1 h at 473 K.

not significantly change the intensity of the 2075-cm^{-1} band; at the same time the multi-bonded species are affected whereas bands at 1595 , 1395 , and 1375 cm^{-1} develop at the expense of the bands due to the HCO_3^- groups (Figs. 7 and 8). Heating at 473 K under hydrogen leads to the disappearance of carbon monoxide molecularly adsorbed on nickel with the formation of methane. After this treatment, the bands at 1595 , 1395 , and 1375 cm^{-1} are still present. They must be attributed to formate species bonded to the Al_2O_3 support according to previous work devoted to the adsorption of methanol or formic acid on oxides (27–30). The intensity of these bands progressively decreases by increasing the temperature of treatment under hydrogen; they disappear after hydrogen reduction at 673 K leading to the formation of additional amounts of methane. After heating at 673 K under hydrogen, a band at 1185 cm^{-1} is observed in the IR spectrum of the resulting sample; this band is no longer observed when the sample is contacted with deuterium at 473 K . The origin of this band will be discussed later.

Ni/MgO catalyst. Carbon monoxide adsorption at 300 K on the Ni/MgO samples gives as for the two previous samples an IR spectrum showing linear and multibonded species. Nevertheless the νCO bands are split; i.e., every linear or multicentered species exhibits multiple IR bands. Bands at 1670 , 1495 , and 1315 cm^{-1} were also observed; they might be assigned to bidentate carbonate groups bonded to the MgO support (30, 31). The introduction of hydrogen at 300 K induces changes in the frequencies of the linear forms and in the value of the ratio of bridged forms to multicentered forms. The carbonate groups were reduced between 300 and 373 K into formate species also bonded to the support and detected by their IR absorptions at 1605 , 1380 , 1360 cm^{-1} . Hydrogen treatment at 473 K leads to the complete transformation of CO adsorbed on Ni into CH_4 , whereas the sample still exhibits formate

groups bonded to the support. As in the case of the Ni/ Al_2O_3 sample, the formate ions are not fully reduced into CH_4 below 673 K .

After heating under hydrogen at 673 K , the IR spectrum shows a band at 1155 cm^{-1} which is shifted to 920 cm^{-1} under deuterium. This band disappears under vacuum at 473 K and is restored under hydrogen at the same temperature. According to inelastic neutron scattering studies (32), this band could be attributed to hydrogen adsorbed on nickel in sites of C_{3v} symmetry. The band at 1185 cm^{-1} observed in the case of the Ni/ Al_2O_3 sample could be attributed to the same species. Its corresponding vibration with deuterium falls in the absorption range of alumina.

The comparison of the IR data with the results of TPH plotted in Fig. 5 leads to the following conclusions. The Ni/ SiO_2 sample does not show any TPH peak at intermediate temperatures (between 523 and 723 K). At the same time, the IR spectrum recorded after hydrogen treatment at 473 K is free of bands ascribable to species linked to the support. On the contrary, the Ni/ Al_2O_3 , Ni/MgO, and Ni-K/ SiO_2 catalysts exhibit TPH peaks at intermediate temperatures. For the Ni/ Al_2O_3 and Ni/MgO solids, IR spectra show the presence of formate groups which are not reduced into CH_4 at temperatures lower than 673 K . Thus the formation of CH_4 between 523 and 723 K in the TPH measurements is connected with the hydrogenation of formate groups bonded to the support. Since the amount of formates increases with the time of reaction, these species are responsible for the large amount of carbon determined on Ni/ Al_2O_3 and Ni/MgO catalysts by chemical analysis (Table 2).

(iii) High Temperature Species

A third type of carbon deposit is only hydrogenated when the temperature is raised to ca. 780 K . This species is mainly detected on Ni/ SiO_2 ; however, it cannot be excluded on the other catalysts. This car-

bon builds up without magnetic interaction ($n = 0$) with the nickel phase since after elimination of the first "active" carbon under hydrogen at 507 K, heating under flowing hydrogen up to 873 K does not alter the saturation magnetization.

This species develops with time of reaction (Table 2): after 15–20 h of reaction, when the sintering is stabilized, its concentration still increases and the catalyst still deactivates. After regeneration of the catalyst by hydrogen treatment at 873 K, a further run produces a new deactivation without sintering and again with the formation of this "high temperature" carbon.

As already pointed out in a previous study (22) this form of stable carbon develops to a higher extent during CO disproportionation than during methanation. At the same time, the overall deactivation appears to be faster and larger for the disproportionation when P_{CO} is increased (Fig. 2). This holds even after having deduced the part of deactivation related to nickel sintering. It may therefore be concluded that this third form of carbon deposit is CO pressure dependent. The simultaneous occurrence of this carbon deposition and of the catalytic deactivation suggests that this species poisons the catalytic surface. Being magnetically noninteracting with the nickel, it could be present as amorphous or graphitic deposits or whiskers, acting as a fouling agent, limiting the access of the reactants to the active nickel sites.

Our results are consistent with previous studies showing that during methanation or disproportionation or steam reforming several types of surface carbon with different reactivity toward hydrogen are formed (21, 33–36). A reactive surface carbon often called C_α is generally considered the intermediate in the methanation process and also the precursor for the catalyst coking (21, 37, 38). It can be transformed at higher temperatures into less reactive species which may encapsulate the Ni crystallites (39).

INFLUENCE OF CO_2 IN THE REACTANT MIXTURE AND ON THE POISONING CARBON SPECIES

The question was whether the deactivation accounted for by high temperature carbon deposition could be limited by adjusting the effluents and not only by raising the H_2/CO ratio. It has been noticed with the Ni–K/SiO₂ sample (Fig. 1) that, when the water gas shift reaction occurs and the selectivity toward CO_2 increases, the deactivation is less marked. A simultaneous decrease in carbon content is observed.

In the present study we have compared the deactivation of the Ni/SiO₂ solid, which has no ability to catalyze the water gas shift reaction, in the absence and in the presence of CO_2 in the reaction gas (mixture $3H_2 + CO$ with 3.1 kPa of CO_2 ; reaction temperature, 507 K). A significantly slower deactivation is observed in the presence of CO_2 (Fig. 9), the sintering being similar for both cases. For identical reaction times the amount of carbon measured from chemical analysis is decreased by ca. 80% in the presence of CO_2 (Table 2). Furthermore, after 20 h of deactivation the temperature-programmed hydrogenation shows that the "high temperature" poisoning carbon species is strongly decreased when the reaction is performed in the presence of CO_2 (Table 2, Fig. 10). The effect of CO_2 in the reactants is therefore to limit the deposition of deactivating carbon. Moreover, these experiments show that the high tempera-

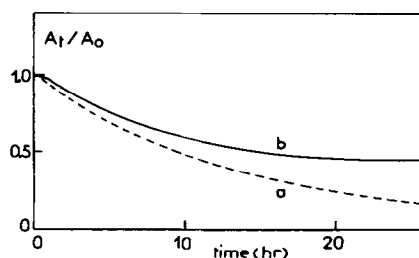


FIG. 9. Ni/SiO₂. Normalized activity A_t/A_0 versus time on stream at 507 K. (a) With the reactant mixture $3 H_2 + CO$; (b) in the presence of CO_2 (3.1 kPa) in the reactant mixture.

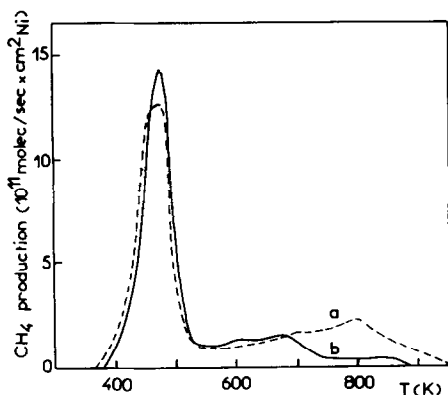
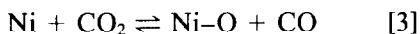


FIG. 10. Ni/SiO₂. Temperature-programmed hydrogenation (8 K min⁻¹) of carbon deposits after methanation during 15 h at 507 K without CO₂ (curve a) and in the presence of CO₂ in the reactant mixture (curve b).

ture peak obtained after reaction without CO₂ is not arising from a conversion of the "active" carbon into an "inactive" species occurring during the hydrogenation treatment itself.

The formation of the "poisoning" carbon being favored by CO and inhibited by CO₂, it could be related to the equilibrium [1] $2\text{CO} \rightleftharpoons \text{CO}_2 + \text{C}$, the latter being displaced according to the changes in either P_{CO} or P_{CO_2} . In order to ascertain this relation, the reactivity of the "poisoning" carbon toward CO₂ has been tested. Ni/SiO₂ was first deactivated under the usual conditions (25 h without CO₂) and then treated overnight in flowing hydrogen at 570 K to eliminate the "active" carbon deposit, already known to react with CO₂ (21). It was then flushed with helium at 507 K and afterward contacted with flowing carbon dioxide at the same temperature. After 1 h of reaction, a large amount of carbon monoxide was detected in the effluent, even exceeding by ca. 40% the amount corresponding to the complete reaction of the poisoning carbon deposit with CO₂. Such an excess probably comes from the dissociation of CO₂ on nickel according to



as proposed in Ref. (21) and checked by

reacting freshly reduced nickel with CO₂ which effectively gives CO and Ni-O (i.e., a decrease in nickel magnetization). However, the main feature is that a much smaller amount of CO is detected when the initial deactivation step is carried out in the presence of CO₂. This amount corresponds roughly to the CO formed from Eq. [3]. It can be therefore concluded that the "poisoning" carbon reacts with CO₂ at the reaction temperature. Since this carbon is not removed by hydrogen treatment at the temperature of reaction, it appears that CO₂ would be kinetically more reactive toward poisoning carbon than molecular hydrogen. This difference in reactivity is rather surprising; further work is necessary to elucidate this behavior.

Our present results appear to be able to elucidate the specific role of CO₂ addition in the methanation feed or the specific resistance to deactivation which is observed for the catalysts which are able to favor the water gas shift reaction, i.e., a production of CO₂ (basic supports or potassium addition). Our interpretation of the CO₂ effect is at variance with other works. For Moeller and Bartholomew (17), on Ni-Mo catalysts which present a similar behavior, the high activity for the water gas shift reaction results in a larger H₂/CO ratio, thereby attenuating the formation of inactive carbon species. Furthermore, the lowering of the deactivation of a Ni-La₂O₃-Ru/SiO₂ composite catalyst in the presence of a low concentration of additional CO₂ is explained by the competitive adsorption of the additive inhibiting the carbon deposition (40). Kuijpers *et al.* (41) have shown that an increased interaction between the Ni particles and the support reduces the formation of filamentous carbon, the "high temperature carbon" being whisker-like. This hypothesis could be taken into account for the Ni/MgO, Ni/Al₂O₃, and Ni-K/SiO₂ systems but cannot explain the behavior of the Ni/SiO₂ sample for the reaction of methanation in the presence of CO₂.

CONCLUSION

By means of *in situ* physical methods (magnetism and infrared spectroscopy) coupled with kinetic measurements, the complex process of deactivation of nickel-based catalysts during low temperature methanation and CO disproportionation has been investigated. The sintering of the nickel phase has been shown to proceed at the first stage of the reaction, being favored by a high initial dispersion and being dependent on the CO pressure. A mechanism via surface carbonyl formation is postulated. The deposition of carbon species in the course of the reaction can be described as follows:

(i) continuous formation of surface nickel carbide Ni_3C which is highly reactive and can either hydrogenate into methane or dissolve into bulk carbide if the hydrogenation is hindered (potassium effect or CO disproportionation);

(ii) reaction of the basic supports like MgO and Al_2O_3 with the methanation reacting or intermediate species for giving carbonate and formate adspecies which are not involved in the deactivating process; and

(iii) build-up of stable carbon species, not interacting magnetically with the nickel, which progressively poison the active nickel surface. These species are in chemical equilibrium with CO and CO_2 , being favored by the former and hindered by the latter.

Thus, the deactivation has been shown to be limited by either adding CO_2 in the methanation feed or using catalysts which favor the WGS reaction (basic supports, potassium addition) and thus produce CO_2 .

Such a specific analysis of each of the various phenomena which contribute to the overall deactivating process should be, in our opinion, carefully achieved before any modeling and optimization of the catalytic deactivation.

REFERENCES

1. van Meerten, R. Z. C., Habets, H. M. J., Beaumont, A. H. G. M., and Coenen, J. W. E., in "New Horizons in Catalysis" (J. Seiyama and K. Tanabe, Eds), p. 1140. Elsevier, Amsterdam/New York, 1980.
2. Shen, W. M., Dumesic, J. A., and Hill, C. G., *J. Catal.* **68**, 152 (1981).
3. Mills, G. A., and Steffgen, F. W., *Catal. Rev. Sci. Eng.* **8**, 159 (1973).
4. Rostrup-Nielsen, J. R., "Steam Reforming Catalysts." Danish Technical Press, Copenhagen, 1975.
5. Trimm, D. L., *Catal. Rev. Sci. Eng.* **16**, 155 (1977).
6. Bartholomew, C. H., *Catal. Rev. Sci. Eng.* **24**, 67 (1982).
7. Wolf, E. E., and Alfani, F., *Catal. Rev. Sci. Eng.* **24**, 329 (1982).
8. Gardner, D. C., and Bartholomew, C. H., *Ind. Eng. Chem. Prod. Res. Dev.* **20**, 80 (1981).
9. Martin, G. A., Imelik, B., and Prettre, M., *J. Chim. Phys.* **66**, 1682 (1969).
10. Praliaud, H., Primet, M., and Martin, G. A., *Appl. Surf. Sci.* **17**, 107 (1983).
11. Turlier, P., Praliaud, H., Dalmon, J. A., and Martin, G. A., in "Proceedings, 5th Intern. Symp. Heterogeneous Catalysis," p. 21. Varna, 1983; Turlier, P., Praliaud, H., Moral P., Martin, G. A., and Dalmon, J. A., *Appl. Catal.* **19**, 287 (1985).
12. Selwood, P. W., in "Chemisorption and Magnetization." Academic Press, New York, 1975.
13. Primet, M., Dalmon, J. A., and Martin, G. A., *J. Catal.* **46**, 25 (1977).
14. Primet, M., to be published.
15. Praliaud, H., Dalmon, J. A., Martin, G. A., Primet, M., and Imelik, B., *C.R. Paris C* **291**, 89 (1980).
16. Praliaud, H., Dalmon, J. A., Mirodatos, C., and Martin, G. A., *J. Catal.* **97**, 344 (1986).
17. Moeller, A. D., and Bartholomew, C. H., *Ind. Eng. Chem. Prod. Res. Dev.* **21**, 390 (1982).
18. Wanke, S. E., and Flynn, P. G., *Catal. Rev. Sci. Eng.* **12**, 93 (1975).
19. Rabo, J. A., and Elek, L. F., "Studies in Surface Science and Catalysis" (T. Seiyama and K. Tanabe, Eds.), Vol. 7, p. 490. Elsevier, Amsterdam, 1981.
20. Martin, G. A., Primet, M., and Dalmon, J. A., *J. Catal.* **53**, 321 (1978).
21. McCarty, J. G., and Wise, H., *J. Catal.* **57**, 406 (1979).
22. Mirodatos, C., Dalmon, J. A., and Martin, G. A., in "Catalysis on the Energy Scene" (S. Kaliaguine and A. Mahay, Eds.), p. 505. Elsevier, Amsterdam, 1984.
23. Kuyjpers, E. G. M., Breedijk, A. K., Van der Wal, W. J. J., and Geus, J. W., *J. Catal.* **81**, 429 (1983).

24. Dalmon, J. A., Primet, M., Martin, G. A., and Imelik, B., *Surf. Sci.* **50**, 95 (1975).
25. Primet, M., Martin, G. A., and Dalmon, J. A., *J. Catal.* **53**, 321 (1978).
26. Parkyns, N. D., *J. Chem. Soc. A*, 410 (1969).
27. Greenler, R. G., *J. Chem. Phys.* **37**, 2094 (1962).
28. Perrichon, V., Pijolat, M., and Primet, M., *J. Mol. Cat.* **25**, 207 (1984).
29. Edwards, J. F., and Schrader, G. L., *J. Phys. Chem.* **89**, 782 (1985).
30. Little, L. H., "Infrared Spectra of Adsorbed Species." Academic Press, London/New York, 1966.
31. Solymosi, F., Erdöhelyi, A., and Bansagi, T., *J. Chem. Soc. Faraday Trans. 1* **77**, 2645 (1981).
32. Jobic, H., and Renouprez, A. J., *J. Chem. Soc. Faraday Trans. 1* **80**, 1991 (1984).
33. Rabo, J. A., Risch, A. P., and Poutsma, M. L., *J. Catal.* **53**, 295 (1978).
34. Kuipers, E. G. M., Jansen, J. W., Van Dillen, A. J., and Geus, J. W., *J. Catal.*, 72 (1982).
35. Gardner, D. C., and Bartholomew, C. H., *Ind. Eng. Chem. Fundam.* **20**, 229 (1981).
36. Bartholomew, C. H., and Vance, C. K., *J. Catal.* **91**, 78 (1985).
37. Wise, H., and McCarty, J. G., *Surf. Sci.* **133**, 311 (1983).
38. Hayes, R. E., Thomas, W. J., and Hayes, K. E., *J. Catal.* **92**, 312 (1985).
39. Gierlick, H. H., Fremery, M., Skov, A., and Rostrup-Nielsen, J. R., in "Catalyst Deactivation" (B. Delmon and G. F. Froment, Eds.), p. 459. Elsevier, Amsterdam, 1980; Rostrup-Nielsen, J. R., *J. Catal.* **27**, 342 (1972); **85**, 31 (1984).
40. Inui, T., Hagiwara, T., and Takegami, Y., *Fuel* **61**, 537 (1982).
41. Kuipers, E. G. M., Tjepkema, R. B., and Geus, J. W., *J. Mol. Cat.* **25**, 241 (1984).